Landes Bioscience www.landesbioscience.com

Supplemental Material to:

Pei-Feng Liu, Chung-Man Leung, Yu-Hsiang Chang, Jin-Shiung Cheng, Jih-Jung Chen, Chung-Jeu Weng, Kuo-Wang Tsai, Chien-Jen Hsu, Yen-Chen Liu, Ping-Chi Hsu, Hung-Wei Pan, and Chih-Wen Shu

ATG4B promotes colorectal cancer growth independent of autophagic flux

Autophagy 2014; 10(8)
http://dx.doi.org/10.4161/auto.29556

www.landesbioscience.com/journals/autophagy/article/29556

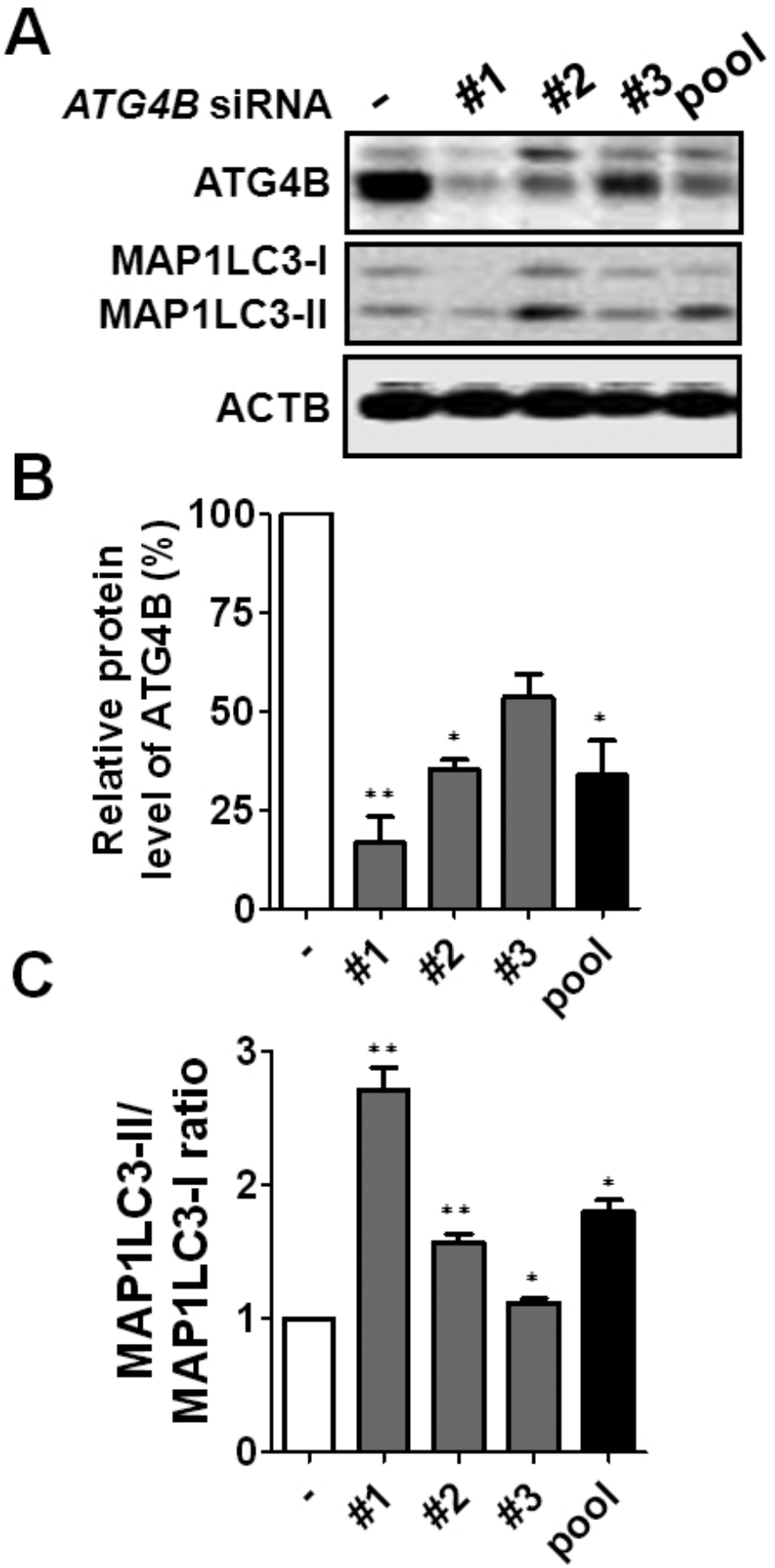
A
ATG4B siRNA
-
#1
#2
#3
pool
ATG4B
MAP1LC3-I
MAP1LC3-II
ACTB
B
Relative protein level of ATG4B (%)
100
75
50
25
0
**
*
*
-
#1
#2
#3
pool
C
MAP1LC3-II/ MAP1LC3-I ratio
3
2
1
0
**
**
*
*
-
#1
#2
#3
pool

Fig. S1

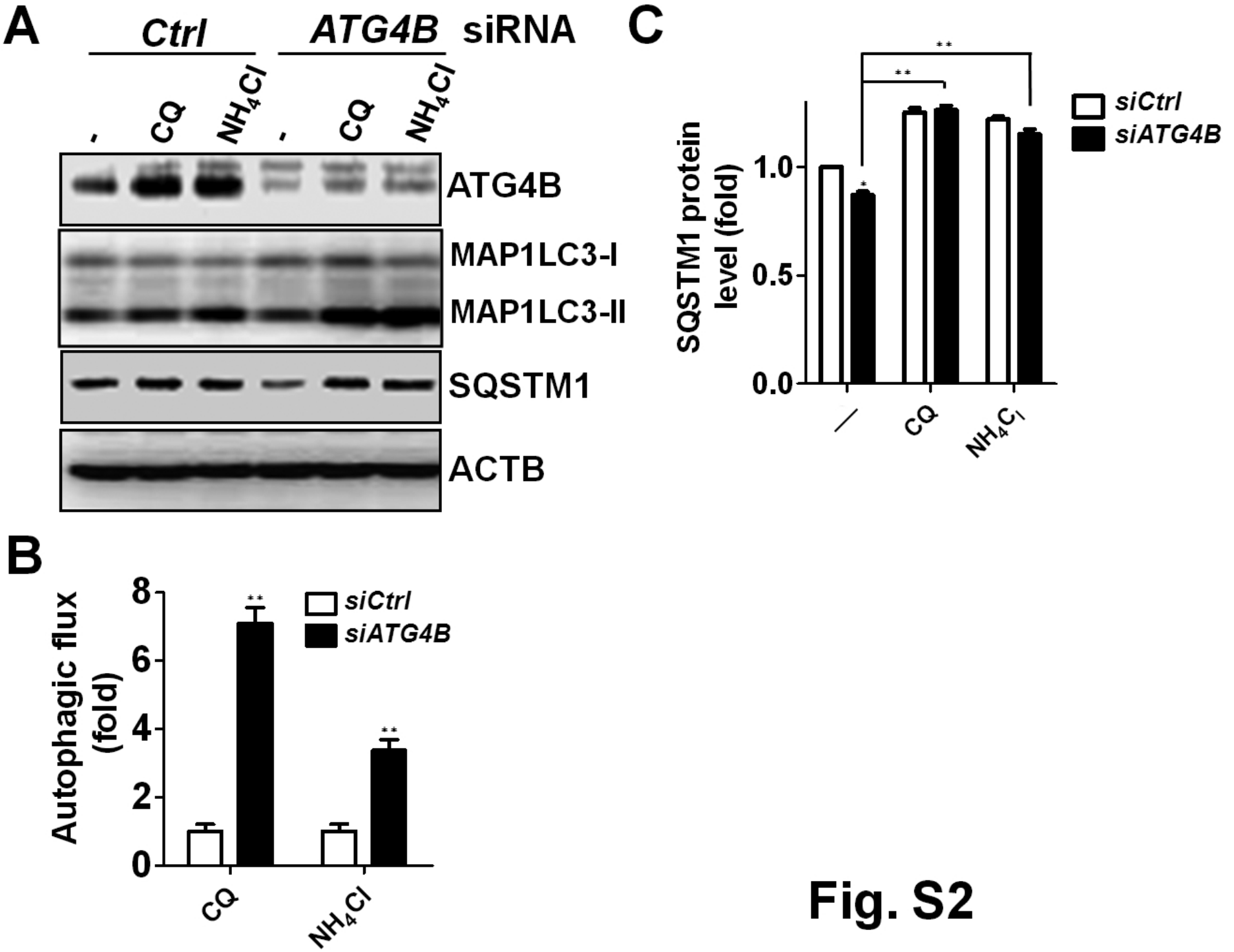
A
Ctrl
ATG4B siRNA
-
CQ
NH4Cl
-
CQ
NH4Cl
ATG4B
MAP1LC3-I
MAP1LC3-II
SQSTM1
ACTB
B
Autophagic flux (fold)
siCtrl
siATG4B
CQ
NH4Cl
C
SQSTM1 protein level (fold)
siCtrl
siATG4B
CQ
NH4Cl

Fig. S2

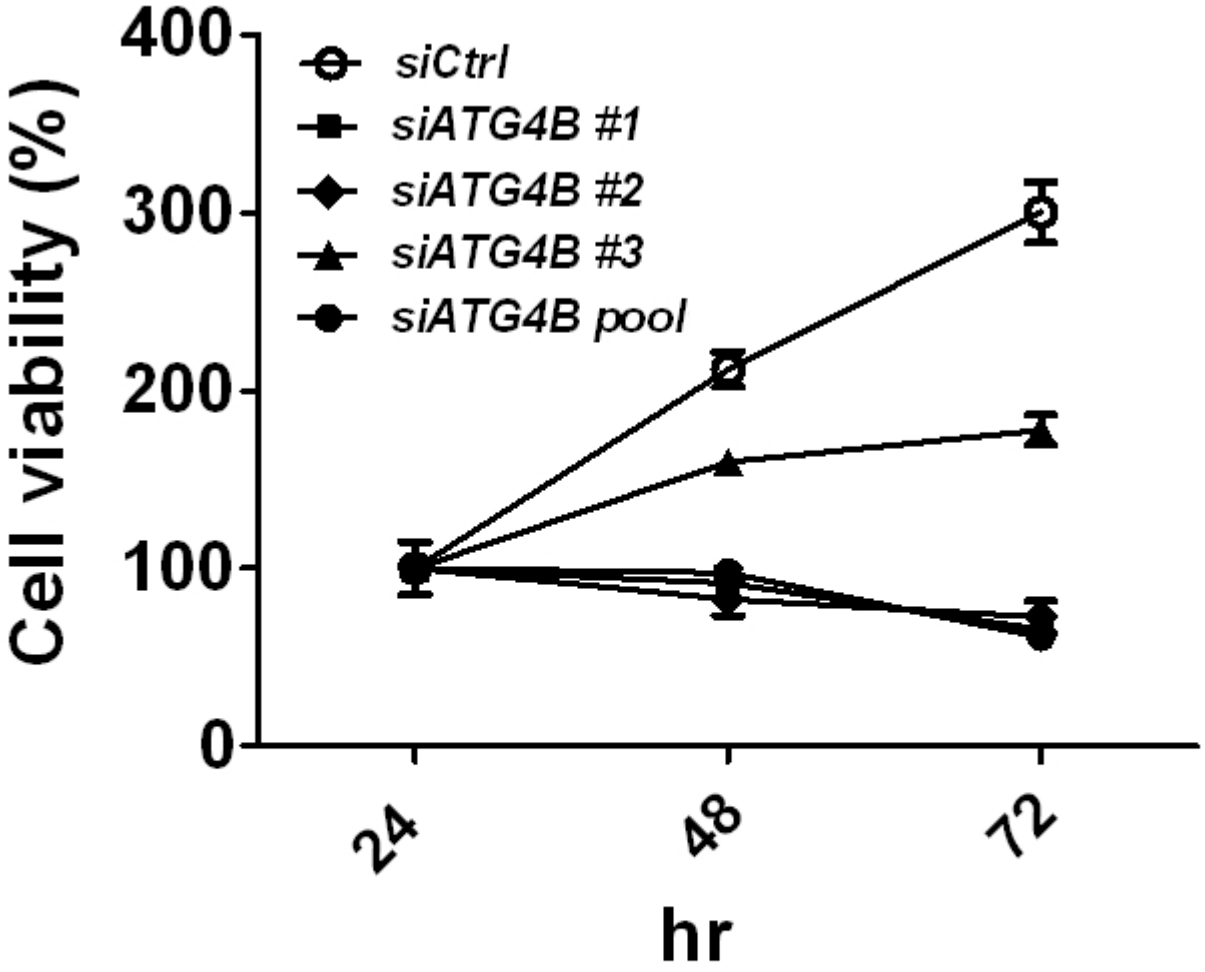
400
300
200
100
0
Cell viability (%)
siCtrl
siATG4B #1
siATG4B #2
siATG4B #3
siATG4B pool
24
48
72
hr

Fig. S3

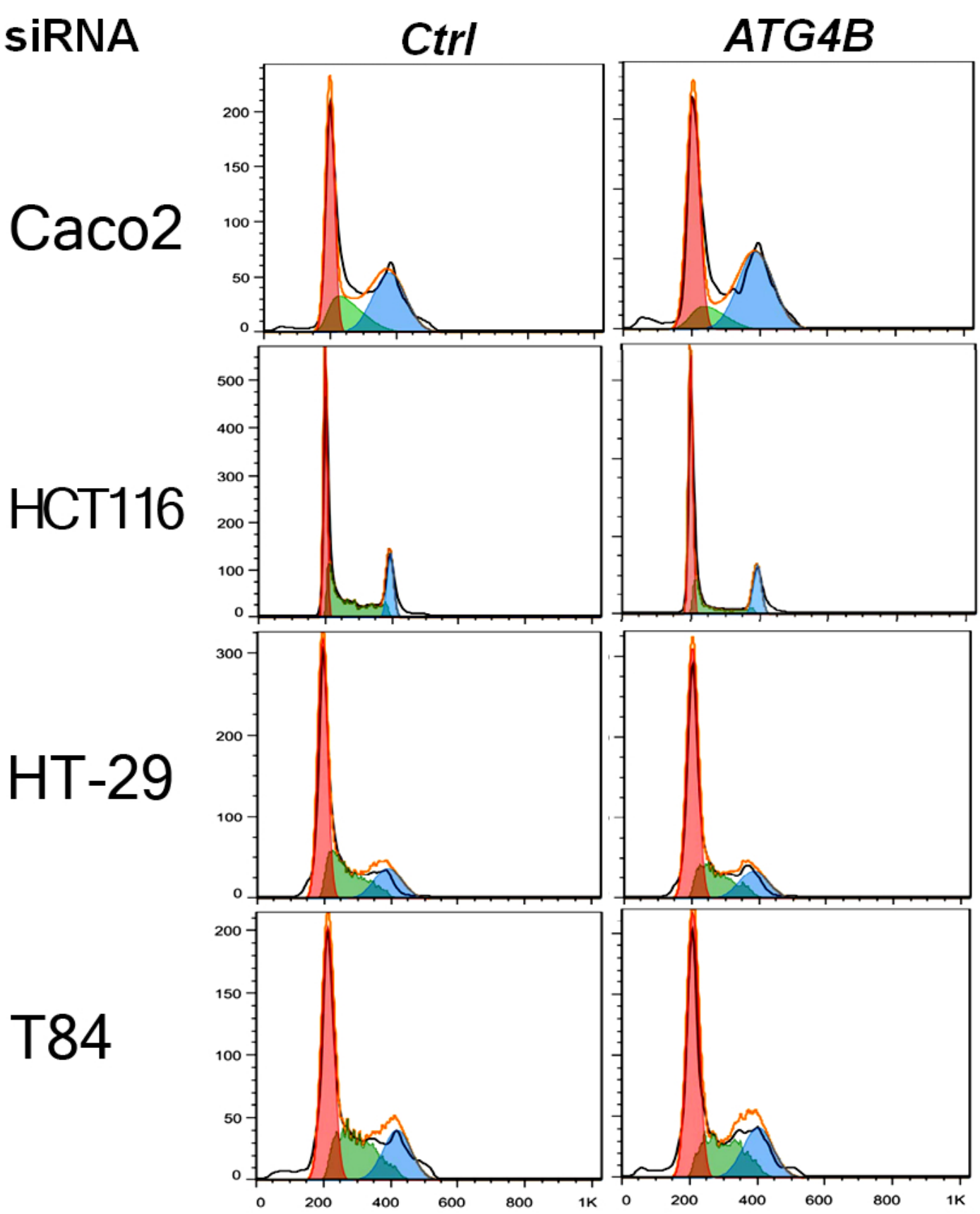
siRNA
Ctrl
ATG4B
Caco2
HCT116
HT-29
T84
0
50
100
150
200
0
100
200
300
400
500
0
100
200
300
0
50
100
150
200
0
200
400
600
800
1K

Fig. S4

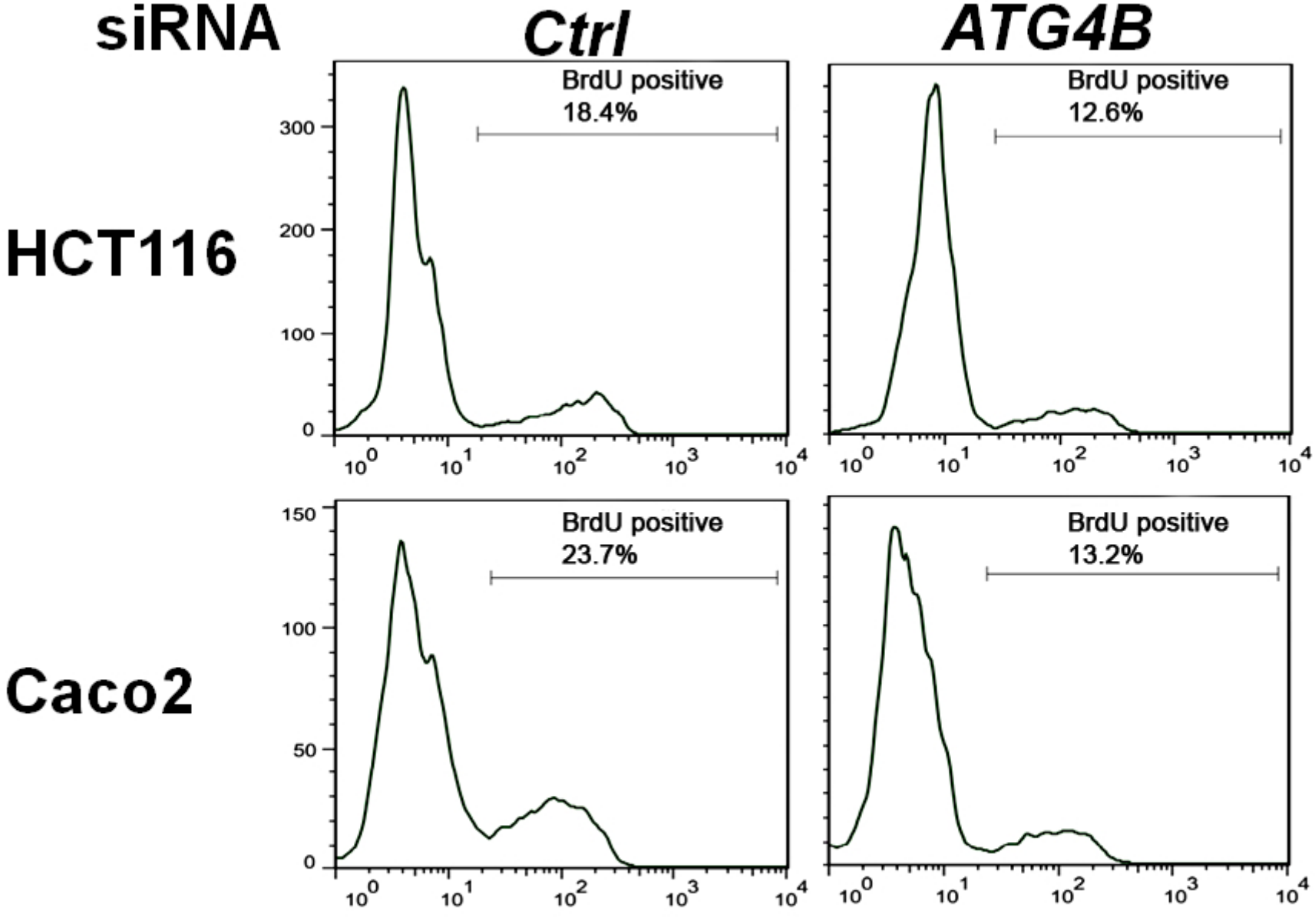
siRNA
Ctrl
ATG4B
HCT116
Caco2
BrdU positive
18.4%
BrdU positive
12.6%
BrdU positive
23.7%
BrdU positive
13.2%

Fig. S5

A

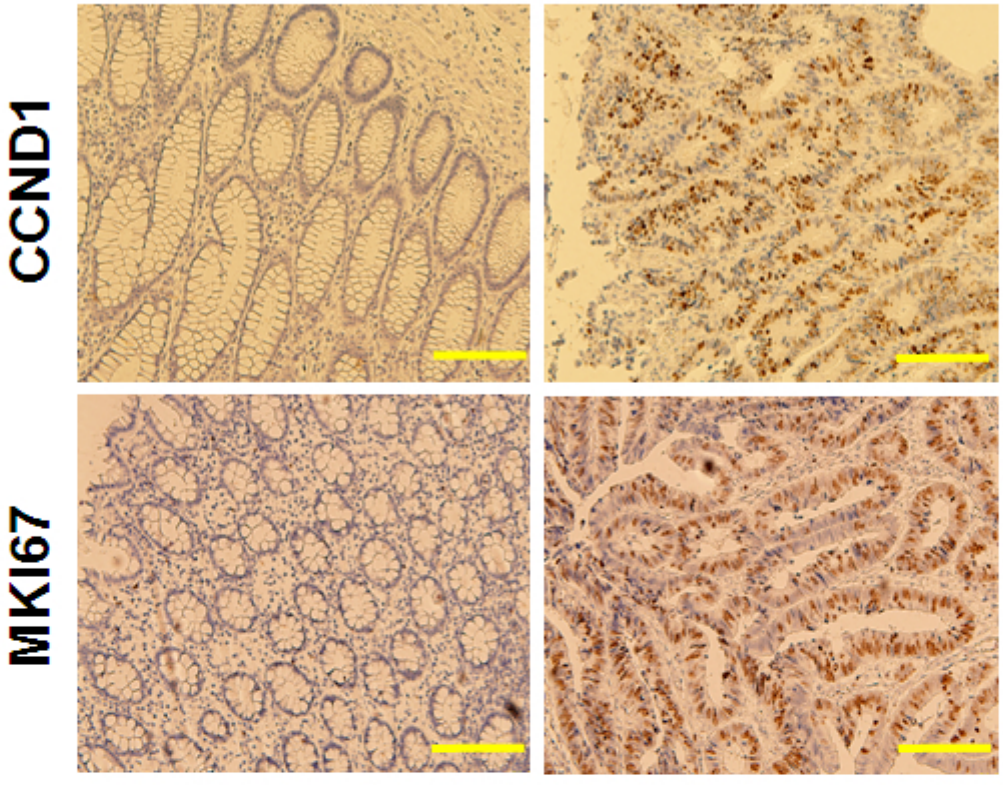

B

N=20	CCND1 expression			
	Negative	Low (score<5)	High (score≧5)	p-value
Normal	20 (100%)	0 (0%)	0 (0%)	<0.001
Tumor	0	9 (45%)	11 (55%)	

N=20	MKI67 expression			
	Negative	Low (score<5)	High (score≧5)	p-value
Normal	20 (100%)	0 (0%)	0 (0%)	<0.001
Tumor	0	12 (60%)	8 (40%)	

Fig. S6

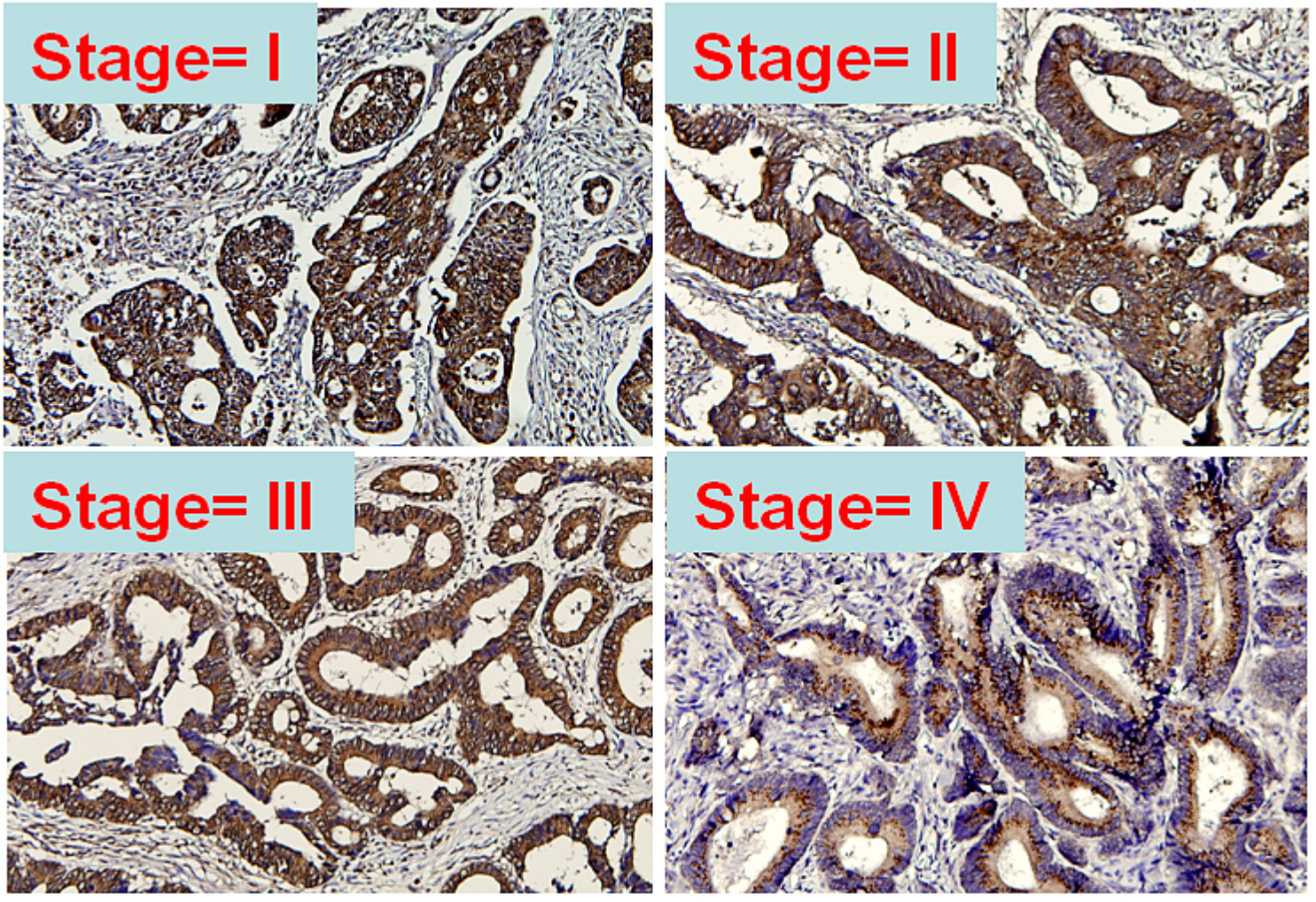

N=20	ATG4B expression	
	Low (IS≦1)	High (IS≧2)
Low Stage (I)	2 (40%)	3 (60%)
High Stage (II~IV)	4 (27%)	11 (73%)

Fig. S7

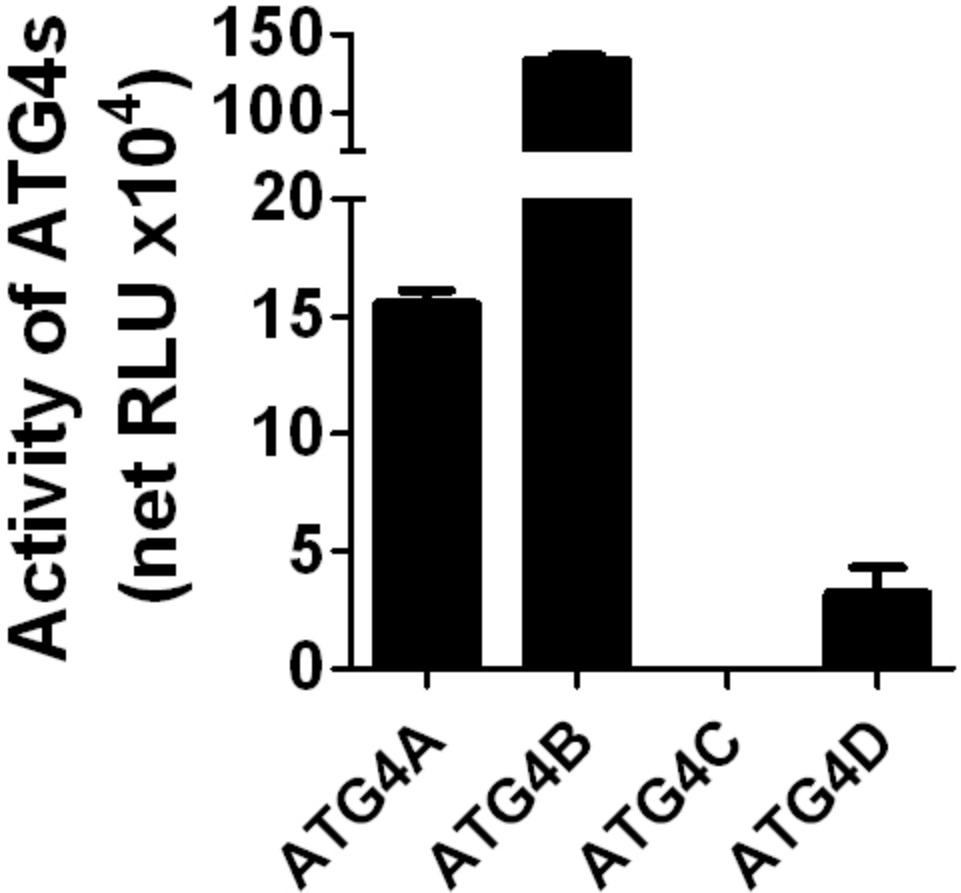
Activity of ATG4s
(net RLU x10^4)
150
100
20
15
10
5
0
ATG4A
ATG4B
ATG4C
ATG4D

Fig. S8

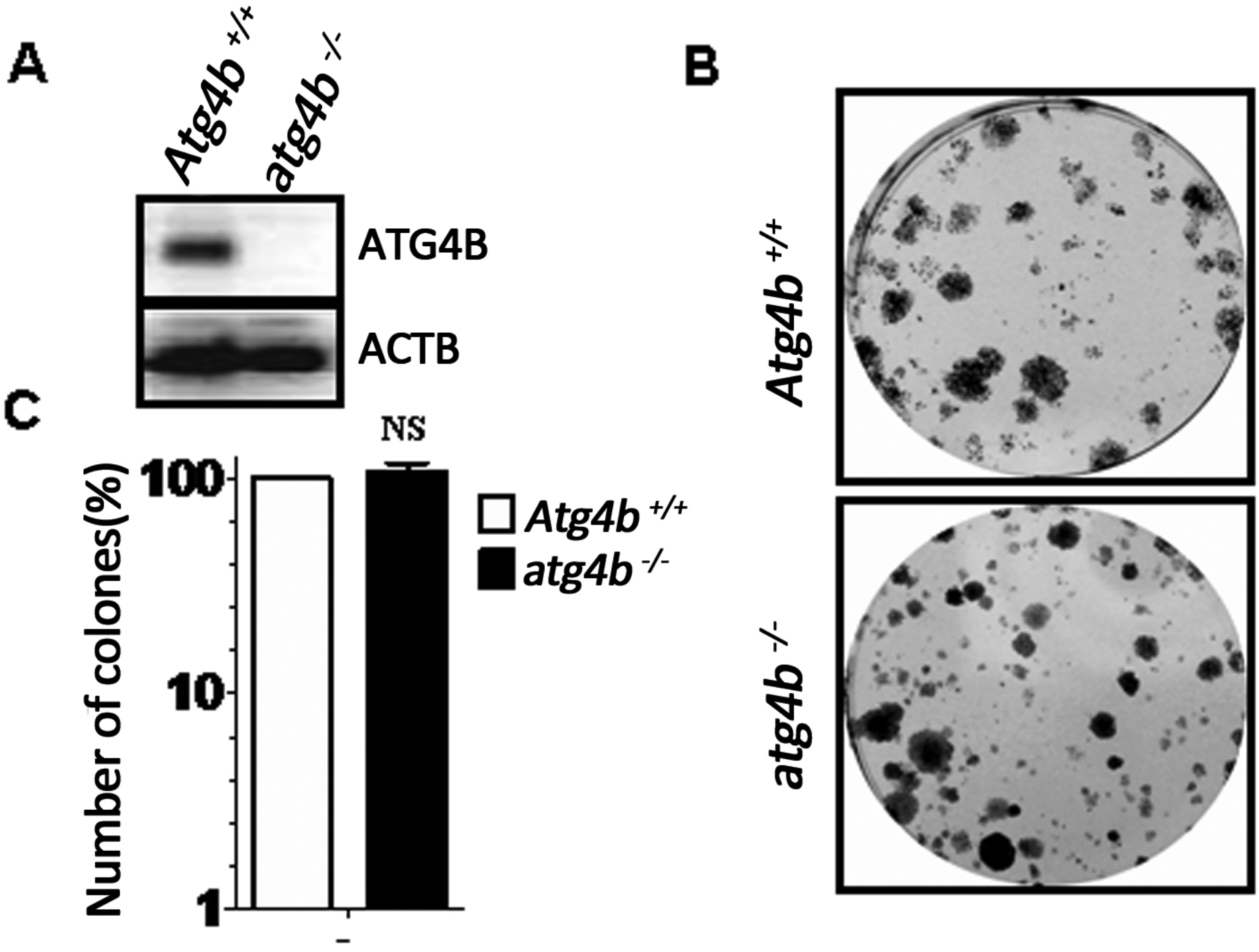
A
Atg4b +/+
atg4b -/-
ATG4B
ACTB
B
Atg4b +/+
atg4b -/-
C
NS
Number of colones(%)
100
10
1
Atg4b +/+
atg4b -/-
-

Fig. S9

Figure S1. Silencing *ATG4B* elevated MAP1LC3-II conversion in human colorectal cancer cells. (**A)** Scrambled siRNA (5 nM, *siCtrl*) or 3 individual siRNAs against *ATG4B* (5 nM, *siATG4B*) was transfected into human colorectal cancer HCT116 cells, and the cells were harvested after 72 h. The cells were lysed for immunoblotting to determine the protein levels of ATG4B, MAP1LC3-I, MAP1LC3-II, and ACTB. (**B)** The knockdown efficiency of ATG4B was quantitated using ACTB as the normalization control. (**C)** The ratio of MAP1LC3-II/MAP1LC3-I as an autophagy marker was employed to determine the effect of silencing *ATG4B* on autophagy. The results are expressed as the mean ± SEM from 3 individual experiments.

Figure S2. Silencing *ATG4B* induced autophagic flux in human colorectal cancer Caco2 cells. (**A)** Human colorectal cancer Caco2 cells were transfected with 5 nM scrambled siRNA (*siCtrl*) or siRNA against *ATG4B* (*siATG4B*) for 72 h and treated with or without (-) 20 μM CQ or 2 mM NH4Cl for 2 h. MAP1LC3-II accumulation and SQSTM1 degradation were examined by immunoblotting to determine the autophagic flux in the *ATG4B*-silenced cells. The level of **(B)** MAP1LC3-II accumulation and **(C)** SQSTM1 degradation in the cells was quantitated. The results are expressed as the mean ± SEM from 3 individual experiments.

Figure S3. Knockdown of *ATG4B* reduced cell viability in a time-dependent manner. Human colorectal cancer HCT116 cells stably expressing luciferase were seeded in 384-well plate in the presence of 5 nM scrambled siRNA (*siCtrl*) or 3 individual (#1, #2, and #3) or pool siRNA against *ATG4B*. The cell viability was measured with 200 μM D-luciferin every 24 h until 72 h. The cells with scrambled siRNA at time 24 h were used for normalization. The results are expressed as the mean ± SEM from 3 individual experiments.

Figure S4. Silencing *ATG4B* arrested the cell cycle at G_1 phase in human colorectal cancer cell lines. Human colorectal cancer HCT116, Caco2, HT-29, and T84 cells were transfected with 5 nM scrambled siRNA (*siCtrl*) or siRNA against *ATG4B* (*siATG4B*) for 72 h. The knockdown cells were fixed and stained with propidium iodide to examine the proportions of the cell cycle by flow cytometry.

The cell cycle profiles were performed from 3 individual experiments and representative data for each cell line are shown.

Figure S5. Silencing *ATG4B* reduced cell proliferation in human colorectal cancer cells. Human colorectal cancer HCT116 (upper panel) or Caco2 (lower panel) cells were transiently transfected with 5 nM scrambled siRNA or siRNA against *ATG4B* for 72 h, followed by a BrdU incorporation assay to determine the role of ATG4B in G_1/S phase progression. The gate is represented as BrdU-positive (S phase) cells. The results shown are representative from 3 individual experiments.

Figure S6. CCND1 and MKI67 expression were elevated in tumor specimens of colorectal cancer patients. **(A)** The expression level of CCND1 and MKI67 in colorectal cancer was determined by immunohistochemistry. Both CCND1 and MKI67 were only expressed in the colorectal tumor cells and not in the adjacent normal tissues (stroma and goblet cells). **(B)** The Allred scoring system was employed to obtain the sum of a proportion score and intensity score for CCND1 and MKI67 protein level. The protein level of CCND1 and MKI67 in the tumor and adjacent normal cells was quantified and are shown in the upper and lower panels, respectively (P<0.001). Twenty tissue samples from colorectal cancer patients were used to determine the protein level. Scale bar: 200 μm.

Figure S7. ATG4B expression was associated with tumor stages of colorectal cancer patients. ATG4B expression at various stages of colorectal cancer was determined by immunohistochemistry. Five tissue samples from colorectal cancer patients for each stage were used to determine the correlation of ATG4B expression with progression of colorectal cancer.

Figure S8. Proteolysis activity of ATG4s on the MAP1LC3-PLA_2 reporter assay. Recombinant ATG4A (5 nM), ATG4B (0.05 nM), ATG4C (50 nM), or caspase-3 (CASP3)-cleaved ATG4D (50 nM) was mixed with 100 nM MAP1LC3B-PLA_2 in the PLA_2 buffer containing 20 μM NBD-C_6-HPC in a total volume of 100 μl. Activation of PLA_2 was monitored with excitation and emission filters of 485 nm and 530 nm, respectively. The results are expressed as the mean ± SEM from 3 individual experiments.

Figure S9. The cell growth rate was similar between *Atg4b*$^{+/+}$ and *atg4b*$^{-/-}$ 3T3 cells. **(A)** The protein expression of ATG4B in *Atg4b*$^{+/+}$ and *atg4b*$^{-/-}$ 3T3 cells was verified by immunoblotting. **(B)** *Atg4b*$^{+/+}$ and *atg4b*$^{-/-}$ 3T3 cells were seeded in 6-well plates at a density of 1 x10^3 cells /ml and grown for 16 d. The cells were fixed and stained with crystal violet for clonogenic assay. **(C)** The colonies were counted, and the data were analyzed using Prism 5.0. The results are expressed as the mean ± SEM from 3 individual experiments.